scientific reports

Check for updates

OPEN

Development of anti-fouling endoscope tip hood for gastrointestinal endoscopy

Yusaku Shimamoto[1,2], Yoshinori Morita[2]✉, Toru Matsunaga[3], Shiori Hino[3], Takao Sato[3], Madoka Takao[1,2] & Yuzo Kodama[1]

The contamination of the endoscope tip lens results in poor endoscopic imaging. To prevent the adsorption of contaminants, we applied a soft contact lens made of 2-hydroxyethyl methacrylate hydrogel to the tip of a gastrointestinal endoscope. Additionally, a novel endoscopic hood with an upper surface composed of a single layer inside the hood cavity was developed. For in vitro anti-fouling performance testing using blood, changes in light transmittance were examined with hydrogel plates and compared to conventional quartz glass and surfactant-coated glass. The transmittance changes at a wavelength of 415 nm were 1.5% for the hydrogel plate, significantly lower than 82.9% for quartz glass and 85.2% for surfactant-coated glass ($p < 0.001$), demonstrating the hydrogel's high anti-fouling performance. Another in vitro quantitative assay, evaluated by exposure to blood, lipid, and mucin liquids, showed high anti-fouling performance in the order hydrogel plate > surfactant-coated glass > quartz glass. Moreover, an in vivo pig model performing gastric endoscopic submucosal dissection was used to evaluate anti-fouling performance by analyzing endoscopic images with Michelson contrast. The contrast value of the upper surface group (Hydrogel) was 0.97, significantly higher than 0.62 for the non-upper surface group (Surfactant) ($P < 0.001$). Therefore, the novel anti-fouling endoscope tip hood could be applied in future clinical applications.

Keywords Medical device, Gastroenterology, Endoscopy

In contemporary medicine, gastrointestinal endoscopy is an essential tool for investigating the interior of the body. The endoscope tip surface is exposed to various contaminants, such as secreted mucus, blood liberated by biopsy procedures, and lipid droplets generated by the damage to submucosal adipose tissue during endoscopic intervention[1,2]. If contaminants adsorbed on the endoscope tip lenses cannot be removed using the water supply function of the endoscope, the endoscope must be removed from inside the body, cleaned, and reinserted, which is time-consuming and a burden on the patient.

Although coating surfactants onto endoscope tip lenses can help prevent fouling[3–5], this is a temporary treatment, and their effectiveness decreases during the endoscopic procedure. To date, there is no adequate solution for maintaining an anti-fouling effect to overcome direct contamination.

Inspired by soft contact lenses, which are made from hydrogel and adhere to the eyeball, we developed a hydrogel hood that fits the endoscope tip. Soft contact lenses are not only highly controlled medical devices to correct vision but also have excellent anti-fouling and anti-fogging properties, and their biosafety is assured. Therefore, we used a soft contact lens made of 2-hydroxyethyl methacrylate (HEMA)[6–10]. This study aimed to evaluate the anti-fouling performance of a hydrogel plate and the feasibility of using this material as a novel endoscope tip hood.

Methods

In vitro analyses

Materials

To evaluate the performance of the anti-fouling properties of HEMA with contaminants expected in gastrointestinal endoscopy, three circular plates with a diameter of 10 mm and thickness of 0.5 mm were prepared: quartz glass (CAS No. 60676-86-0), lens-cleaning surfactant-coated quartz glass, and a hydrogel plate.

[1]Division of Gastroenterology, Department of Internal Medicine, Kobe University Graduate School of Medicine, Kobe, Japan. [2]Division of Gastroenterology, International Clinical Cancer Research Center, Kobe University, 1-5-1, Minatojima minami machi, Chuo-ku, Kobe 650-0047, Japan. [3]Department of Research and Development, Seed Co., Ltd., Tokyo, Japan. ✉email: ymorita@med.kobe-u.ac.jp

Cleash (Fujifilm Co., Tokyo, Japan) was used as a lens-cleaning surfactant. The hydrogel plates were prepared using HEMA (CAS No. 868-77-9) with a 38% water content. The plates were immersed in ultrapure water and sterilized by high-pressure steam sterilization at 121 °C for 30 min. For the contaminants, three different liquids were prepared: (1) whole rabbit venous blood (SLC, Inc., Japan) to mimic bleeding from mucosal injury; (2) a lipid mixture containing 2.83 g lecithin, 0.06 g oleic acid, 0.06 g linoleic acid, 0.06 g palmitic acid, 0.81 g tripalmitin, 0.08 g cholesterol palmitate, 0.08 g cholesterol, 0.20 g cetyl alcohol, and 0.81 g cetyl myristate to simulate submucosal adipose exposure; and (3) mucin derived from porcine stomach (CAS No. 84082-64-4) to represent gastric or intestinal secretions.

Contamination experiments

To measure light transmittance, one side of the circular plate was masked with tape and placed in a well (Fig. 1). Then, 500 µL of whole blood was poured into the well and shaken for 1 min at room temperature. The circular plate was then rinsed with water and dried for 2 min. This was defined as one cycle.

The quantification assay was also performed without masking the plate. In this case, 500 µL of whole blood was poured into the well and shaken for 1 min at room temperature. For the lipid mixture or 10% (v/v) mucin, 2 mL of liquid was poured into the well and shaken for 30 min at 37 ℃.

Light transmittance measurements

The masking tape was removed from the circular plate contaminated with whole blood (three contamination cycles), which was then dried for 24 h at room temperature. The light transmittance was measured using a spectrophotometer (V-750, JASCO Corporation, Tokyo, Japan) focused on the most contaminated area of the circular plate. The transmittance was measured in steps of 5 nm in the 220–800 nm range. The visible-light transmittance was calculated by defining the average of transmittances in the 380–780 nm range. The visible-light transmittance changes were defined as the transmittance of the pre-performed blank plate minus that of the sample plate. Anti-fouling performance was defined as the property of the material with the lowest transmittance change values.

Total protein quantification assay

Circular plates contaminated with whole blood or mucin during contamination experiments were placed in a test tube, along with 2 mL of an extract solution consisting of 1.0% (v/v) sodium dodecyl sulfate and 1.0% (v/v) sodium carbonate. The mixtures were ultrasonicated for 60 min, and then the circular plates were removed from the test tube. The 1 mL of liquid remaining in the test tube was then used to quantify the total protein levels with a Pierce™ BCA Protein Assay Kit (Thermo Scientific, 23225) relative to a BSA standard for blood experiment and self-purified mucin for a mucin experiment. The color intensity was measured at 562 nm using a spectrophotometer (V-750, JASCO Corporation, Tokyo, Japan).

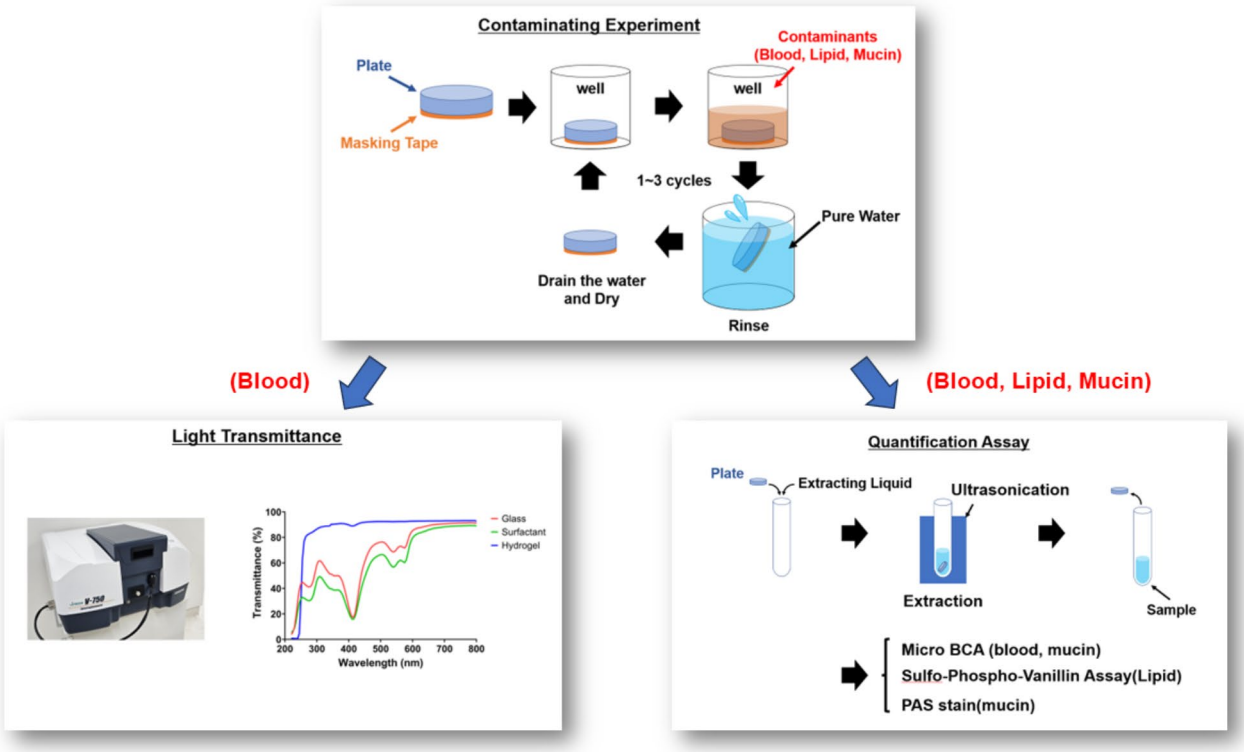

Fig. 1. Schematic of in vitro experiments.

Quantitative PAS assay
A quantitative periodic acid/Schiff stain (PAS) assay was used to detect carbohydrates on mucin-contaminated circular plates[11]. Using 96-well plates, 50 µL of the samples extracted using a total protein quantification assay was pipetted into a well and incubated with 120 µL of 0.06% (v/v) periodic acid diluted in 7% (v/v) acetic acid for 90 min at room temperature. Then, 100 µL of Schiff's stain (Muto Pure Chemicals, 40931) was added, and the solutions were incubated for another 60 min at room temperature. The absorption was measured at 550 nm after 5 s of shaking (Varioskan LUX, Thermo Scientific). Self-purified mucin was used as the standard.

Total lipid quantification assay
The circular plates contaminated with the lipid mixture after the contamination experiments were placed in a test tube, and 1 mL of a 3:1 mixture of ethanol and diethyl ether was pipetted into the tube. After vortexing, the circular plates were immersed at room temperature for 30 min. The circular plates were removed from the test tube, and the remaining liquid was evaporated to dryness. Concentrated sulfuric acid (2 mL) was added to the test tube and incubated at 90 °C for 10 min. After vortexing, 1 mL of each sample was transferred to a new test tube. Then, 5 mL of a 4:1 mixture of phosphoric acid and 0.6% (v/v) vanillin solution was added, and the resulting mixture was incubated at 37 °C for 15 min. The color intensity was measured at 525 nm using a spectrophotometer (V-750, JASCO Corporation, Tokyo, Japan). Self-purified olive oil was used as the standard.

In vivo analyses

Study design
These experiments were conducted to evaluate the anti-fouling performance and feasibility of a novel endoscope tip hood consisting of HEMA in an in vivo pig model (Fig. 2). The experimental protocol was approved by the Institutional Animal Care and Ethical Review Board (IVTeC Co., Ltd. Animal Welfare Committee). All methods were performed in accordance with the relevant guidelines and regulations. This study was conducted in accordance with the ARRIVE guidelines.

Animals and devices
In vivo experiments were performed using two Clawn miniature pigs (Kagoshima Miniature Swine Research Center, Kagoshima, Japan): 39 months old (40 kg) and 52 months old (54 kg). The animals underwent two days of fasting, general anesthesia with endotracheal intubation, and monitoring. The experiments were conducted using an EG-580RD gastroscope (Fujifilm Corporation, Tokyo, Japan) with a hydrogel hood made by HEMA at the tip. For this endoscope tip hood, a resin mold replicating the structure of the endoscope tip was created, and HEMA was injected into the mold to polymerize and swell. The upper surface structure of the endoscope tip was designed to ensure compatibility with the endoscope, aligning the respective hole for the upper surface and the corresponding channels at the endoscope tip for a fixed and secure fit. Two types of hoods were fabricated for this study: one with an upper surface layer covering the endoscope tip lens and another without any part covering

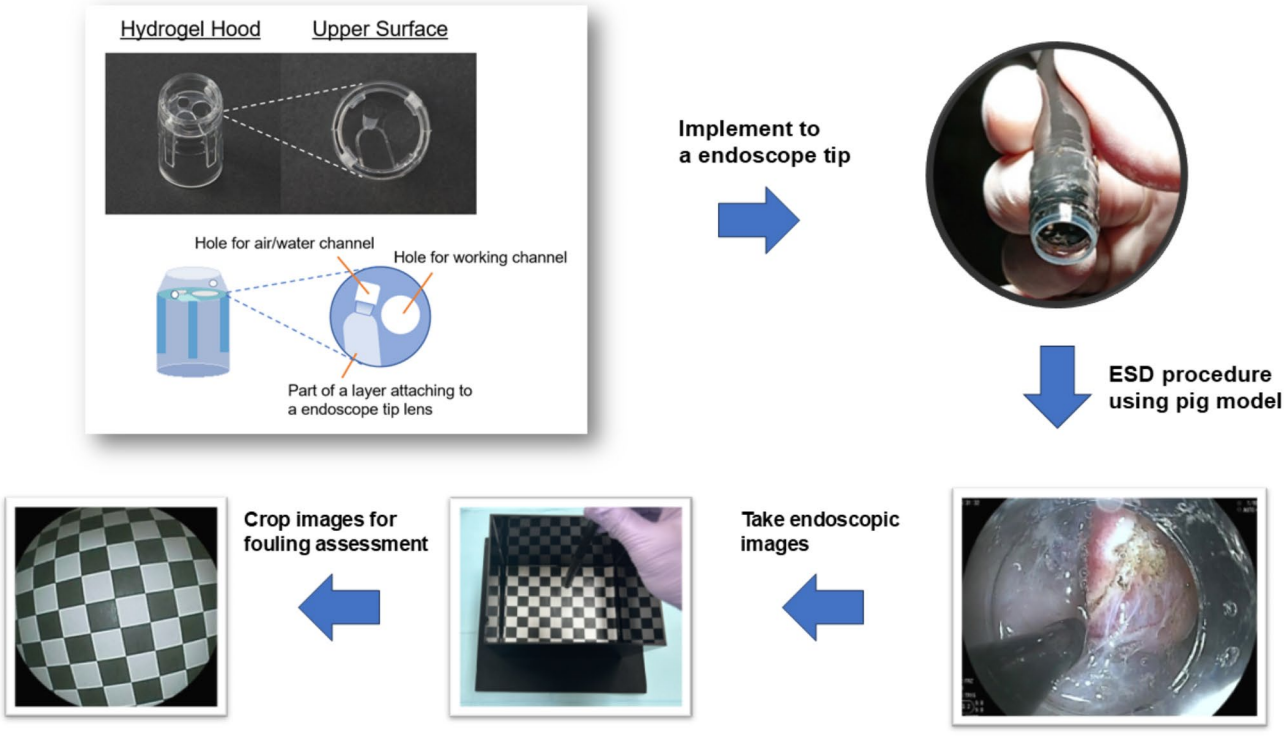

Fig. 2. Schematic of in vivo experiments.

the lens, consisting only of a cylindrical hydrogel hood. The outer frame of both hood types, excluding the upper surface, was identical, with no structural or functional differences. Both types of hoods were immersed in ultrapure water and sterilized by high-pressure steam sterilization at 121 °C for 30 min. As a result, two groups of hydrogel hoods were used to study the effect of the anti-fouling performance: the upper surface group (Hydrogel) and the non-upper surface group (Surfactant). In the non-upper surface group (Surfactant), the endoscope tip was treated with Cleash surfactant (Fujifilm Co., Tokyo, Japan) after attaching a cylindrical hydrogel hood. The endoscope tip hoods in both groups were fixed to the endoscope using tape. A high-frequency generator (VIO 200 S, ERBE, Germany) was used for endoscopic submucosal dissection (ESD). In addition, hydrogel hoods were single-use and discarded after each ESD procedure and replaced by a new one.

ESD procedure

Ten simulated circular lesions (2.0–2.5 cm in diameter) were made in the stomach of each pig, six in the gastric body, and four in the antrum. The ESD was performed by two endoscopists (Y.S. and Y.M.). For the ESD procedure, saline was used for submucosal injection. Circumferential mucosal incision and submucosal dissection were then performed using either the Flush knife BT (Fujifilm Medical, Tokyo, Japan) or IT knife 2 (Olympus, Tokyo, Japan) at the discretion of the operator, depending on the stomach region and lesion situation. The ESD procedure time was defined as the time from the insertion of the injection needle until the complete removal of the lesion. After ESD, the amount of water used was measured using a water bottle connected to the endoscope. After pinning the resected lesions onto a board, the lengths of the longer and shorter axes were measured. The specimen area (mm^2) was calculated using the following elliptical formula: specimen area = ([shorter axis length]/2) × ([longer axis length])/2) × 3.14.

Fouling assessment based on endoscopic images

Soon after ESD was performed, the endoscope was placed into a black box (height = 15 cm, width = 22 cm, length = 18 cm) to evaluate the fouling of the endoscope tip. Holding the tip of the endoscope at a height of 10 cm from the bottom of the box, the endoscope was used to capture images of a black-and-white checkerboard pattern on the bottom of the box. To blind the evaluation, ImageJ/Fiji software was used, and the centers of the endoscopic images were cropped to a circular area of $5.0 \times 10^5 \pm 1.0 \times 10^4$ pixels. A fouling assessment was performed using subjective and objective methods. As a subjective evaluation based on previous reports[4,12,13], fouling of the endoscopic images was evaluated on a five-point scale: grade 0: entire image is clear; grades 1, 2, 3, 4, and 5: ~10%, > 10% to < 50%, ~ 50%, > 50% to < 100%, and almost all of the image, respectively, is unclear. The evaluation was performed by two endoscopists (Y.S. and Y.M.); if there was a disagreement, discussions were held, and one of the grades was selected. As an objective evaluation, Michelson contrast was used to determine the visibility. The Michelson contrast= $(I_{max}\text{-}I_{min})/(I_{max}+I_{min})$, where I_{max} and I_{min} represent the highest and lowest brightness, as determined by ImageJ/Fiji software over the most fouled 2 × 2 checkerboard area of an image.

Outcome measurements

The aim of this study was to evaluate the anti-fouling performance of hydrogel materials in a simulated gastrointestinal endoscopic environment. The anti-fouling performance was evaluated the in vitro examinations using bloods, lipid mixtures, and mucins, and the in vivo examination of ESD procedure using pig model. Then, the primary outcomes were defined as objective quantitative anti-fouling performances. For the in vitro evaluations, the light transmittance change (blood) and the contaminant levels (protein, lipid mixture, and mucin) were assessed, while Michelson contrast values was used for the in vivo evaluation. Secondary outcomes were in vivo semi-quantitative visual fouling score, procedural efficiency (procedure time, water usage), safety metrics (perforation), and resection accuracy (En bloc resection, specimen area).

Statistical analysis

Statistical analysis was performed using the Student's t-test or Mann-Whitney U test. The Kruskal–Wallis test was performed, followed by Bonferroni post-hoc testing for multiple comparisons. Statistical significance was set at $P < 0.05$. All statistical analyses were performed using GraphPad Prism 9.0.

Results

Light transmittance assessment of blood contamination

The light transmittance was examined to evaluate blood contamination. A reddish hue was observed when the quartz glass and surfactant-coated glass plates were contaminated with blood with increasing treatment cycles (Fig. 3a). However, the hydrogel plates showed no clear contamination. After three cycles of blood contamination, the obtained light transmittance spectra show similar features to that of the hemoglobin absorption spectra (Fig. 3b). The light transmittance change was analyzed at three specific wavelengths (415 nm, 540 nm, and 580 nm) as well as the average transmittance across the visible spectrum (380–780 nm) (Table 1). At 415 nm, the transmittance change was 1.5% for the hydrogel group, which was significantly lower than 82.9% for the quartz glass group and 85.2% for the surfactant-coated glass group ($p < 0.001$). Transmittance changes at 540 nm, 580 nm, and the average across 380–780 nm also showed that the hydrogel group exhibited the lowest transmittance change compared to the quartz glass and surfactant-coated glass groups. However, multiple comparison tests revealed no significant differences for these measurements.

Quantitative assessment of contaminants (blood, lipid, and mucin)

For blood contamination, there was no significant difference among the three groups during cycle 1. However, in cycle 2, the hydrogel group exhibited the lowest blood contaminants, with significantly lower values than the

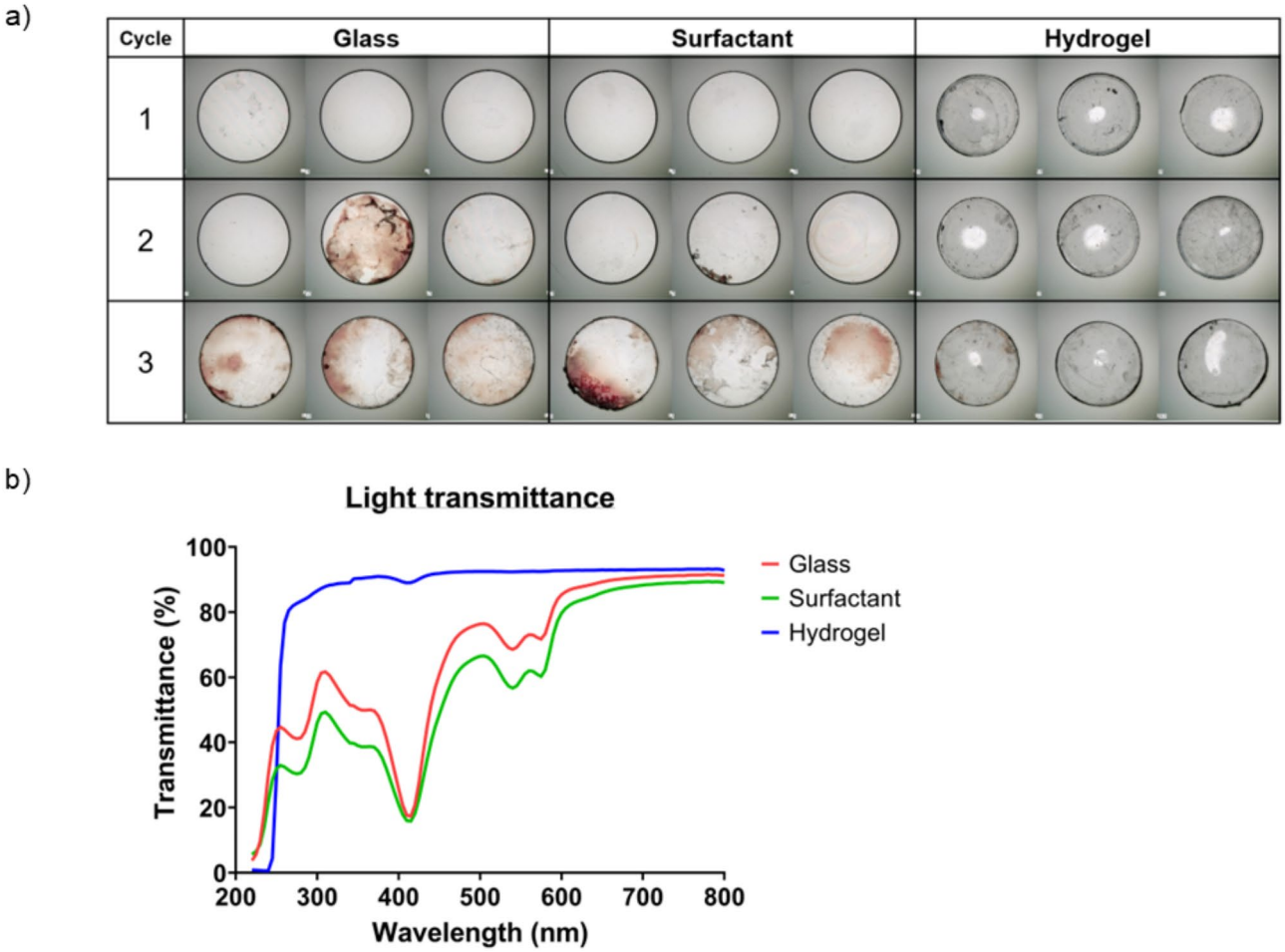

Fig. 3. In vitro anti-fouling performance against contaminants. (**a**) Microscopy images of the quartz glass, surfactant-coated glass, and hydrogel plates after each cycle of blood contamination. (**b**) Light transmittance spectra of blood-contaminated samples after three contamination cycles ($n = 3$).

surfactant-coated glass group ($p = 0.047$) (Table 1). Furthermore, in cycle 3, the hydrogel group again showed the lowest blood contaminants, with significantly lower values than the quartz glass group ($p = 0.006$). For lipid contamination, in every cycle, the total lipid contamination followed the order: quartz glass > surfactant-coated glass > hydrogel plate. All pairwise comparisons among the groups showed significant differences. For mucin contamination, both the BCA and PAS assays displayed trends similar to those observed for blood and lipid. In the BCA assay, during cycle 1, the hydrogel group exhibited the lowest mucin contaminants, with significantly lower values than the quartz glass group ($p = 0.007$). In cycle 2, the hydrogel group had the lowest mucin contaminants, but the difference was not statistically significant. By cycle 3, mucin contaminants in the hydrogel group were significantly lower than those in the quartz glass and surfactant-coated glass groups ($p = 0.008$). Similarly, in the PAS assay, during cycle 1, the hydrogel group had the lowest mucin contaminants and significantly lower values than the quartz glass group ($p = 0.007$). In cycle 2, mucin contaminants were again lowest in the hydrogel group, but the differences were not statistically significant. By cycle 3, the hydrogel group had significantly lower mucin contaminants compared to both the quartz glass group ($p = 0.002$) and the surfactant-coated glass group ($p = 0.003$).

ESD for endoscope tip Hood assessment in the pig model

The novel hydrogel endoscopic hood was evaluated using ESD in a pig model. In both the non-upper and upper surface groups, all lesions achieved En bloc resection with no perforation. Furthermore, in both groups, no cases required scope withdrawal for lens cleaning. No significant differences in the specimen area and water usage were observed between the groups (Fig. 4a, b). For the fouling assessment, a subjective evaluation was performed with a defined criterion (Fig. 4c); the upper surface group (Hydrogel) had a median value of 0, which was significantly lower than the non-upper surface group (Surfactant) of 3.0 ($P = 0.002$) (Fig. 4d). Moreover, the objective evaluation resulted in Michelson contrast values for the upper surface group (Hydrogel) were significantly higher with a median of 0.97 compared to 0.62 for the non-upper surface group (Surfactant) ($P < 0.001$) (Fig. 4e), which also showed a significantly shorter procedure time than the non-upper surface group (Surfactant) (Fig. 4f).

		Glass ($n=5$)	Surfactant ($n=5$)	Hydrogel ($n=5$)	p-value (Unadjusted)	Glass vs. Surfactant	Glass vs. Hydrogel	Surfactant vs. Hydrogel
						p-value (Bonferroni Adjusted)		
Light transmittance change								
Blood, % ($n=3$)	415 nm	82.9 (71.1–82.9)	85.2 (71.9–88.0)	1.5 (0.8-6.0)	< 0.001	1	< 0.001	< 0.001
	540 nm	32.4 (17.6–32.4)	37.8 (24.7–50.5)	0.5 (0.2–1.3)	0.097	1	0.384	0.126
	580 nm	26.7 (14.0-26.7)	30.5 (19.7–43.6)	0.4 (0.2–1.7)	0.121	1	0.484	0.157
	average (380–780 nm)	16.5 (13.1–24.5)	28.0 (18.4–39.0)	1.0 (0.8–1.7)	0.071	1	0.461	0.150
Quantitative assay								
Blood, μg	Cycle 1	2.4 (1.7–34.4)	0 (0–0)	5.7 (5.6-8.0)	0.127	0.140	0.735	1
	Cycle 2	76.8 (64.4-124.9)	82.7 (80.0-82.7)	11.6 (7.5–14.7)	0.027	1	0.064	0.047
	Cycle 3	227.8 (103.2-242.8)	90.9 (67.7–90.9)	18.8 (16.8–46.8)	< 0.001	0.171	0.006	0.269
Lipid, μg	Cycle 1	36.2 (33.7–42.5)	10.9 (10.4–12.7)	2.4 (2.0-2.7)	< 0.001	< 0.001	< 0.001	0.038
	Cycle 2	60.0 (59.8–68.1)	39.2 (33.3–46.1)	5.9 (4.3–7.7)	< 0.001	0.044	< 0.001	0.002
	Cycle 3	116.5 (91.0-119.2)	76.4 (69.2–80.2)	4.3 (3.9-5.0)	< 0.001	0.001	< 0.001	< 0.001
Mucin (BCA assay), μg	Cycle 1	276.6 (221.6–289.0)	171.7 (75.4-211.5)	82.0 (71.2–96.4)	0.008	0.174	0.007	0.302
	Cycle 2	260.6 (187.0-312.7)	205.3 (114.5-223.9)	138.8 (76.5-156.4)	0.050	0.307	0.053	1
	Cycle 3	246.1 (159.7-426.2)	290.1 (218.9–358.0)	42.1 (32-54.7)	0.003	1	0.008	0.008
Mucin (PAS assay), μg	Cycle 1	377.5 (328.6-402.9)	259.8 (184.2-316.5)	147.7 (135.3-167.3)	0.007	0.185	0.007	0.277
	Cycle 2	343.9 (257.2-389.9)	276.7 (173.4-295.2)	203.3 (118.5–248.0)	0.056	0.352	0.059	1
	Cycle 3	349.0 (250.2-454.6)	345.6 (267.3-421.7)	55.3 (50.5-115.7)	< 0.001	1	0.002	0.003

Table 1. Comparison of three materials exposed to contaminants. Values are presented as median (IQR, interquartile range). BCA, bicinchoninic acid; PAS, periodic acid/Schiff stain.

Discussion

The anti-fouling performance of the hydrogel plate was demonstrated through in vitro experiments. Quartz glass was used as a high-transmittance optical lens for the endoscope tip. However, glass readily adsorbs charged proteins and lipids exposed during endoscopic procedures, and contaminants accumulate as they are strongly adsorbed on the lens surface[14–16]. Amphiphilic coatings on endoscopic tip lenses have been investigated and implemented in clinical practice to overcome this problem[3–5]. However, the water supply function of the endoscope removes the surfactant, and the limitations of this solution are more pronounced with severe endoscopic procedures. To provide a better solution, we applied a hydrogel endoscope tip lens composed of a hydrophilic material to provide sustainable anti-fouling performance[8,10]. The in vitro contamination experiments showed that the hydrogel plate maintained better anti-fouling performance with repeated exposure to contaminants compared to quartz glass (with and without a surfactant coating).

An in vivo pig model was used to evaluate the anti-fouling performance and the feasibility of the hydrogel endoscope tip hood with an upper-surface structure developed to fit the selected endoscope tip. ESD is widely performed as a less invasive intervention to treat superficial gastrointestinal neoplasms with a low risk of metastasis[17–21]. However, owing to the characteristics of the resection method, submucosal dissection results in hemorrhage and the scattering of lipid droplets, as well as various cell necrotic substances by electrocoagulation. Hence, ESD is one of the most challenging procedures for the endoscope tip, often resulting in poor-quality imaging[22]. Unclear endoscopic images are stressful for the operator and can increase the risk of perforation complications[2,22]. In the current study, all ESD procedures were performed by En bloc resection without perforation. The upper surface group (Hydrogel) maintained clear endoscopic images after ESD, as determined by subjective and objective assessments, and a short procedure time was achieved. On the other hand, water usage was higher in the upper surface group (Hydrogel) compared to the non-upper surface group (Surfactant). This difference may be attributed to the thickness of the upper surface, which could prevent contaminants from being adequately washed away in the upper surface group (Hydrogel). However, the difference in water usage between the two groups was not statistically significant and did not impact the procedure. Additionally, while the hydrogel hood in the current study is intended for single use, the hydrogel material, HEMA, is widely used in soft contact lenses and is relatively inexpensive. Therefore, Cost feasibility remains comparable to that of existing endoscopic hoods. Therefore, the in vivo experiments demonstrated the anti-fouling performance and feasibility of the novel endoscope tip hood.

The light transmittance was measured as an indicator of blood contamination. Erythrocytes, also known as red blood cells, constitute the largest cell population in blood and include hemoglobin proteins. This protein exhibits specific spectrophotometric wavelengths[23], corresponding to the absorption maxima for oxyhemoglobin at 415, 542, and 578 nm; de-oxy-hemoglobin at 430 and 560 nm; and methemoglobin at 405 and 603 nm. Our light transmittance results for the quartz glass and surfactant-coated glass groups showed peaks consistent with the absorption maxima of oxyhemoglobin. Therefore, the light transmittance evaluation method

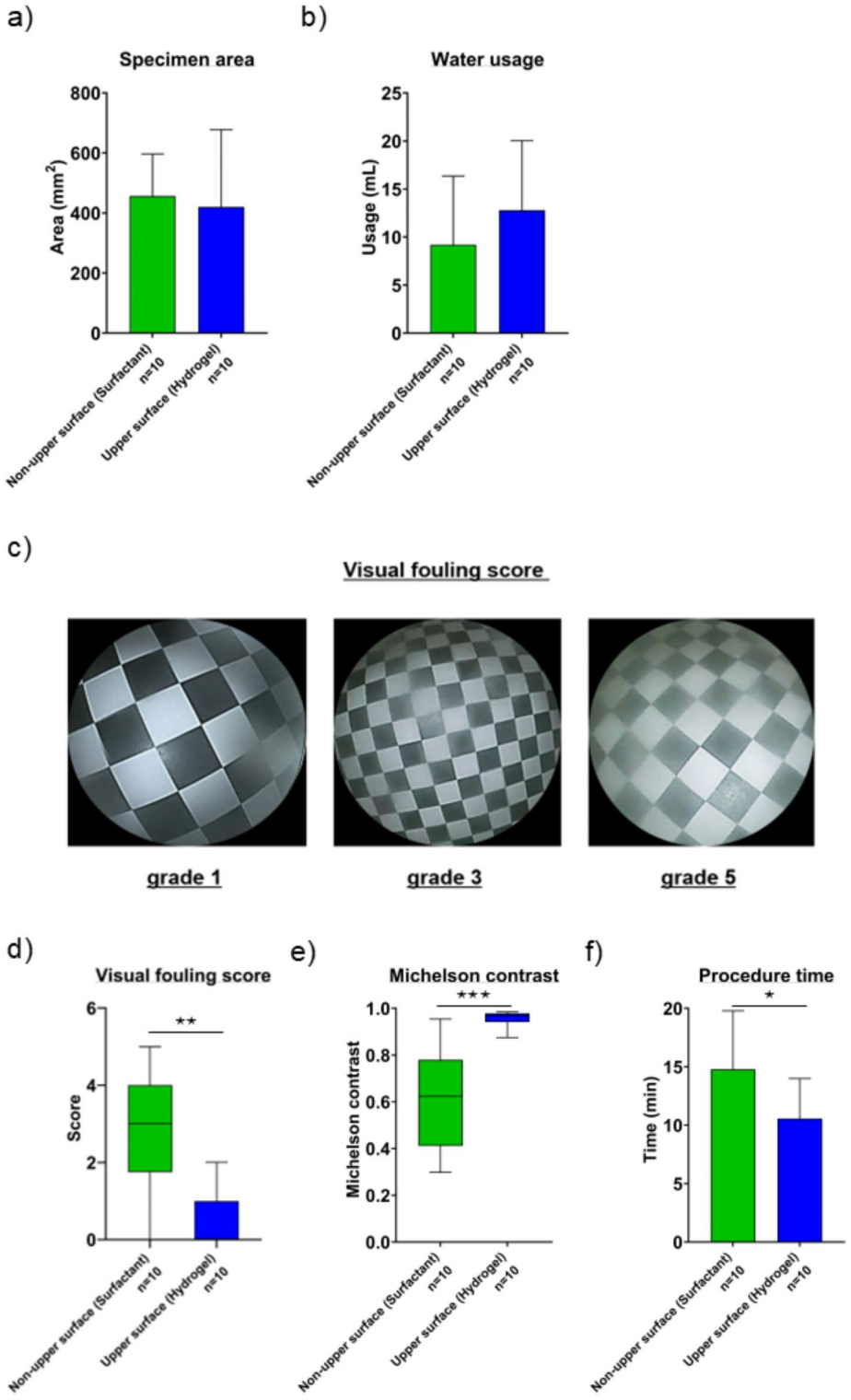

Fig. 4. Anti-fouling performance of endoscope tip hood for in vivo pig model. (**a**) Area of resected specimens for the non-upper surface (Surfactant) and upper surface groups (Hydrogel). (**b**) Water usage during ESD. (**c**) Visual fouling score (grades 1, 3, and 5) of the endoscopic images. (**d**) Visual fouling scores of the obtained endoscopic images. (**e**) Michelson contrast was calculated from the brightness measured by ImageJ/Fiji. (**f**) ESD procedure time. Data are expressed via mean + standard deviation or standard box and whiskers of $n = 10$ independent experiments. *p-value < 0.05; **p-value < 0.01; ***p-value < 0.001.

is considered appropriate for identifying blood contamination and showed that the hydrogel plate tended to be less contaminated among the three groups.

This study has several limitations. The in vitro experiments simulated the gastrointestinal environment using blood, lipid mixtures, and mucin. However, these conditions cannot fully replicate the complexity of in vivo environments, such as interactions with tissues, enzymes, and dynamic fluids. Additionally, the blood contamination experiments were conducted at room temperature to prevent coagulation, which may have influenced the results compared to experiments conducted at physiological temperature (37℃). Additionally, the upper surface within the hood structure was specifically designed for the endoscope used in this study. The basic structure of the endoscope tip consists of an optical lens and two holes for air/water and working channel. Adjacent to the hole for the air/water channel, a sloped surface is designed to effectively direct water for cleaning the optical lens. While many endoscopes follow this basic structure, their surface designs vary slightly from one another. However, hydrogel hoods are fabricated using resin molds, which can be manufactured and adapted to accommodate different endoscope tip shapes. This flexibility allows hydrogel hoods to be easily customized for endoscopes of various designs. Furthermore, the in vivo experiments were not blinded, introducing the potential for operator bias in subjective evaluations. Finally, the ESD procedures in the current study were relatively short, and the durability of the hydrogel hood under prolonged exposure to high-temperature environments, as encountered during large lesion resections, was not evaluated. This aspect warrants further investigation to assess long-term performance.

In the current study, the anti-fouling performance of a novel endoscope tip hood was evaluated through both in vitro and in vivo experiments. The in vitro results demonstrated that the hydrogel plate exhibited superior anti-fouling performance compared to quartz glass and surfactant-coated glass. Moreover, the in vivo experiments confirmed the anti-fouling performance of the hydrogel hood in applications involving ESD. However, further evaluation in actual clinical practice is required. Additionally, expanding the application of the hydrogel hood to emergency endoscopic procedures, where the endoscope tip is frequently exposed to food residue, should also be considered.

Data availability

All data generated or analyzed during this study are included in this published article.

Received: 12 October 2024; Accepted: 25 February 2025
Published online: 25 April 2025

References

1. Saito, I. et al. Complications related to gastric endoscopic submucosal dissection and their management. *Clin. Endosc*. **47**, 398–403 (2014).
2. Ramos-Zabala, F. et al. The impact of submucosal fatty tissue during colon endoscopic submucosal dissection in a Western center. *Eur. J. Gastroenterol. Hepatol.* **33**, 1063–1070 (2021).
3. Komazawa, Y. et al. Oolong tea is useful for lens cleansing in transnasal small-caliber Esophagogastroduodenoscopy. *Endoscopy* **42**, 104–108 (2010).
4. Yoshida, N. et al. Risk of lens cloudiness during colorectal endoscopic submucosal dissection and ability of a novel lens cleaner to maintain and restore endoscopic view. *Dig. Endosc*. **27**, 609–617 (2015).
5. Fujii, T. et al. Analysis of lens cloudiness during endoscopic submucosal dissection procedures: Effects of a novel lens cleaner. *DEN Open.* **5**, e416 (2025).
6. Chirila, T. V. Melanized poly(HEMA) hydrogels: Basic research and potential use. *J. Biomater. Appl.* **8**, 106–145 (1993).
7. Wheeler, J. C. et al. Evolution of hydrogel polymers as contact lenses, surface coatings, dressings, and drug delivery systems. *J. Long. Term Eff. Med. Implants*. **6**, 207–217 (1996).
8. Luensmann, D. & Jones, L. Protein deposition on contact lenses: The past, the present, and the future. *Cont. Lens Anterior Eye*. **35**, 53–64 (2012).
9. Bishop, S. & Roberts, H. Methacrylate perspective in current dental practice. *J. Esthet Restor. Dent.* **32**, 673–680 (2020).
10. Zare, M. et al. pHEMA: An overview for biomedical applications. *Int. J. Mol. Sci.* 22 (2021).
11. Kilcoyne, M., Gerlach, J. Q., Farrell, M. P., Bhavanandan, V. P. & Joshi, L. Periodic acid-Schiff's reagent assay for carbohydrates in a microtiter plate format. *Anal. Biochem.* **416**, 18–26 (2011).
12. Knauth, A., Weiss, M., Dave, M., Frotzler, A. & Haas, T. Comparison of antifog methods in endoscopy. What really helps. *Anaesth* **61**, 1036–1044 (2012).
13. Komazawa, Y. et al. Effectiveness of solution with 5% detergent for cleaning transnasal Esophagogastroduodenoscopy lens. *Clin. Endosc*. **54**, 236–241 (2021).
14. Sunny, S. et al. Transparent anti-fouling material for improved operative field visibility in endoscopy. *Proc. Natl. Acad. Sci. U. S. A*. **113**, 11676–11681 (2016).
15. Tatsuki, H. et al. A novel one-step lens cleaning device using air and water flow for endoscopic surgery. *PLoS ONE*. **13**, e0200749 (2018).
16. Lee, Y. et al. Lubricant-infused directly engraved nano-microstructures for mechanically durable endoscope lens with anti-biofouling and anti-fogging properties. *Sci. Rep.* **10**, 17454 (2020).
17. Uedo, N. et al. Longterm outcomes after endoscopic mucosal resection for early gastric cancer. *Gastric Cancer*. **9**, 88–92 (2006).
18. Takeuchi, Y. et al. Endoscopic submucosal dissection with insulated-tip knife for large mucosal early gastric cancer: A feasibility study (with videos). *Gastrointest. Endosc*. **66**, 186–193 (2007).
19. Oka, S. et al. Advantage of endoscopic submucosal dissection compared with EMR for early gastric cancer. *Gastrointest. Endosc*. **64**, 877–883 (2006).
20. Chung, I. K. et al. Therapeutic outcomes in 1000 cases of endoscopic submucosal dissection for early gastric neoplasms: Korean ESD study group multicenter study. *Gastrointest. Endosc*. **69**, 1228–1235 (2009).
21. Al Ghamdi, S. S. & Ngamruengphong, S. Endoscopic submucosal dissection in the stomach and duodenum: Techniques, indications, and outcomes. *Gastrointest. Endosc Clin. N Am*. **33**, 67–81 (2023).
22. Imagawa, A. et al. Endoscopic submucosal dissection for early gastric cancer: Results and degrees of technical difficulty as well as success. *Endoscopy* **38**, 987–990 (2006).
23. Karabaliev, M., Tacheva, B., Paarvanova, B. & Georgieva, R. Change in osmotic pressure influences the absorption spectrum of hemoglobin inside red blood cells. *Cells* **13** (2024).

Author contributions

Y.S., Y.M., T.M., S.H., T.S., M.T., and Y.K. designed the study. Y.S. analyzed the data and wrote the original draft. All authors approved the final submitted draft.

Funding

This study was funded by the Japan Agency for Medical Research and Development (grant number 21he0122001j0002).

Declarations

Competing interests

Toru Matsunaga, Shiori Hino and Takao Sato are employees of Seed Co., Ltd.All the remaining authors declare no conflict of interest.

Additional information

Correspondence and requests for materials should be addressed to Y.M.

Reprints and permissions information is available at www.nature.com/reprints.

Publisher's note Springer Nature remains neutral with regard to jurisdictional claims in published maps and institutional affiliations.